

On the Development of Two Models to Produce Reliable Operational Snowfall Estimates

Mike Huston - NOAA/NWS Forecast Office Pocatello, Idaho

1. INTRODUCTION

Snowfall observations across southeast Idaho are sporadic in nature and vary widely with regard to accuracy, coverage, and timeliness. Official snowfall measurements have been recorded at the Pocatello National Weather Service (NWS) office on a 6- and 24-hour basis since 1939. Additional observations are collected through the NWS Cooperative Observer Program (COOP) covering a 24-hour observational period at varying times of the day while the Community Collaborative Rain, Hail, and Snow (CoCoRaHS) volunteer network can span any number of time-scales. To compound matters, no automated platforms, outside of a handful of Snow Telemetry (SNOTEL) sites equipped with acoustic sounding devices, report snowfall directly. The vagaries between these systems allow for little if any intercomparison or consistent reporting of snowfall over time and space. In an effort to overcome these shortfalls, the present work seeks to reformulate the widely discarded New Snowfall to Estimated Meltwater Conversion Table (hereafter referred to as MCT; U.S. Department of Commerce 1996; NWS Observing Handbook No. 7) while also developing an Ordinary Least Squares (OLS) regression model in the hope that either or both of these models might prove useful in conjunction with output from automated meteorological platforms in producing reasonably accurate, timely, and consistent snowfall estimates in an operational setting.

2. DATA

The Kühtai automated data set (Krajci et al. 2017) was selected for use in this study due to its longevity, quality, availability, and concomitant manual snow depth measurements. The site is located approximately 30 km (19 mi) west of Innsbruck, Austria at an elevation of 1920 m (6299 ft) MSL and 47 degrees north latitude in an Alpine climate roughly similar to that found in the northern Rockies which borders a large portion of southeast Idaho. Of primary use here were the automated 15-min snow water equivalent (SWE), water equivalent precipitation (Pcprn), incoming shortwave radiation, air temperature (T), relative humidity, wind speed and direction, and ultrasonic snow depth (SND) meteorological data, as well as the the 0700 LT manual snow depth measurements (SNDM) taken at the observation site each day. Gross quality control (QC) measures were also applied by the custodial agency during initial post processing of the data (Krajci et. al. 2017).

Due to the limitations associated with the 24-hour manual snow depth measurements taken at the observation site, a daily summary file ending at 0700 LT was constructed from the 15-minute meteorological data. The 24-hour change in SNDM and the maximum daily change in SND were both used as proxies for new snowfall. Visual inspection of days with new snowfall revealed noticeable event-to-event snowfall (SNDM) variability among similar Pcprn-SWE days (not necessarily a bad thing) while a smaller number of days exhibited noticeable intraday elemental incongruities, possibly associated with questionable or errant data values. Much of the event-to-event variability could have been plausibly explained by common meteorological processes

noted during the observational period such as wind or melting. Since the thrust of this study was intended to develop a model that could produce reliable operational snowfall estimates, cases displaying destructive post-snowfall meteorological processes, namely wind, wind packing, radiational melting, sublimation, and exaggerated settling were removed from the formal analysis although displayed in the figures throughout the model development process. Normal melting processes associated with warm ambient temperatures during the snowfall events were included in the analysis in order to provide a seamless thermal model for snowfall. Records that were deemed unintelligible were not included in the analysis and were labeled as OtherSnw in the figures. Every effort was made to retain salvageable data.

Entwined in the general culling process described above and based on the need to address some of the interelemental incongruities observed in the data, each record was subjected to a circuitous “optimizing” technique. During a preliminary workup on a smaller subset of data, an MCT-like table was created. The table was subsequently used to produce snowfall estimates based on the observed Pcpn, SWE, and Average of the Pcpn and SWE in conjunction with the average temperature (Tavg) observed during the snowfall events. These MCT-like estimated snowfall values were then compared to the observed SNDM and SND values. The combination of variables and associated snowfall estimates producing the most coherent (or “Best”) match with the observed snowfall values (SNDM or SND) were retained for further analysis.

3. MODEL SPECIFICATION

A broad body of research has been conducted over the years regarding cold-cloud precipitation processes and the development, growth, and modification of snow crystals and resulting quantitative snowfall. Cobb and Waldstreicher (2005) provide an excellent synopsis and background of much of this work which will not be repeated here other than to note that atmospheric temperature, moisture, and vertical motion as well as spatial and orographic effects (Judson and Doesken 2000) play a complex role in the snowfall process. Given the limitations associated with the surface-based observational Kühtai data set, only a narrow subset of this body of work will be considered in this study.

A. Preliminary Data Survey

Prior to the culling and optimizing process described in section 2, all available meteorological variables (independent variables) captured in the Kühtai data set where the maximum daily temperature was below freezing were compared to SNDM (dependent variable) to see if any visible correlations were evident that might prove useful in the redevelopment of the MCT and in the specification of an OLS model. The comparisons that showed promising results are presented below.

The related variables of Pcpn, SWE, and the Average of the Pcpn and SWE data each showed similar results. Figure 1 is a traditional depiction of a fitted line plot for the 24-hour change in snow depth (SNDM) (dependent variable) versus the Average of Pcpn & SWE (independent variable). The accompanying regression statistics indicated that the independent variable accounted for over 67% of the variance ($r^2=0.671$) in the dependent variable with a standard error of the

regression (S) of a little over 1.9 in (5.0 cm). It was also evident that questionable data was present within the sample given the number of observations showing high values of water equivalent precipitation and correspondingly low SNDM (see red oval in Fig. 1) for days where the maximum daily temperature was below freezing.

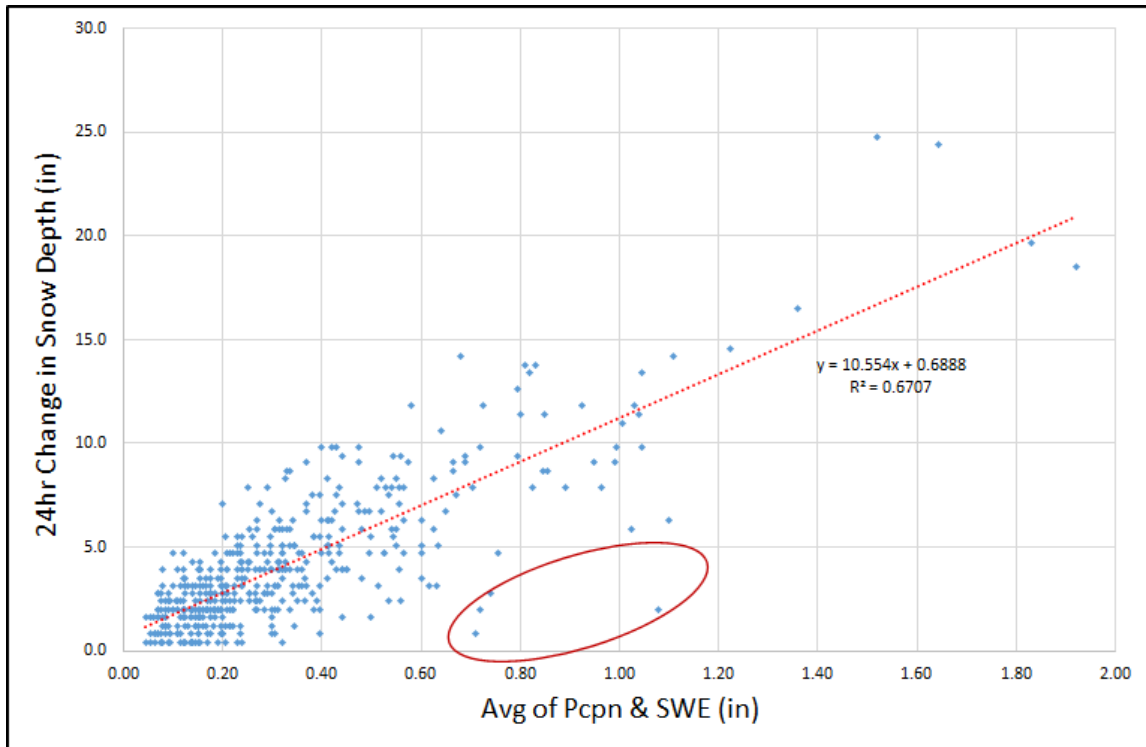


Figure 1. Avg of Pcpn & SWE vs the 24-hour Change in Snow Depth (SNDM). $r^2=0.671$, Adjusted $r^2=0.670$, $S=1.953$, $p\text{-value}=1.4E-111$. Potential QC issues highlighted within the red oval.

A plot of the residuals (Fig. 2) showed a clear case of heteroscedasticity - a fan shape or unequal scatter in the residuals. For now, it is important to understand that heteroscedasticity does not produce bias but it can adversely impact the precision of regression coefficients in an OLS model if not addressed. It can also produce p-values that are smaller than they would otherwise be, leading one to conclude that a regression term is statistically significant when it may not be. This issue will be treated in much greater detail in Section 3.C where the development of an OLS regression equation will be covered.

The next variable that was expected to show a promising relationship was temperature. At first blush, Figure 3 appears to show little if any relationship between snowfall and the average temperature ($r^2 = 0.017$). But upon closer inspection, a number of interesting details emerge.

The first item of interest is the apparent peak in the 24hr change in snow depth occurring with a surface temperature falling roughly between -5.6 and -3.3°C

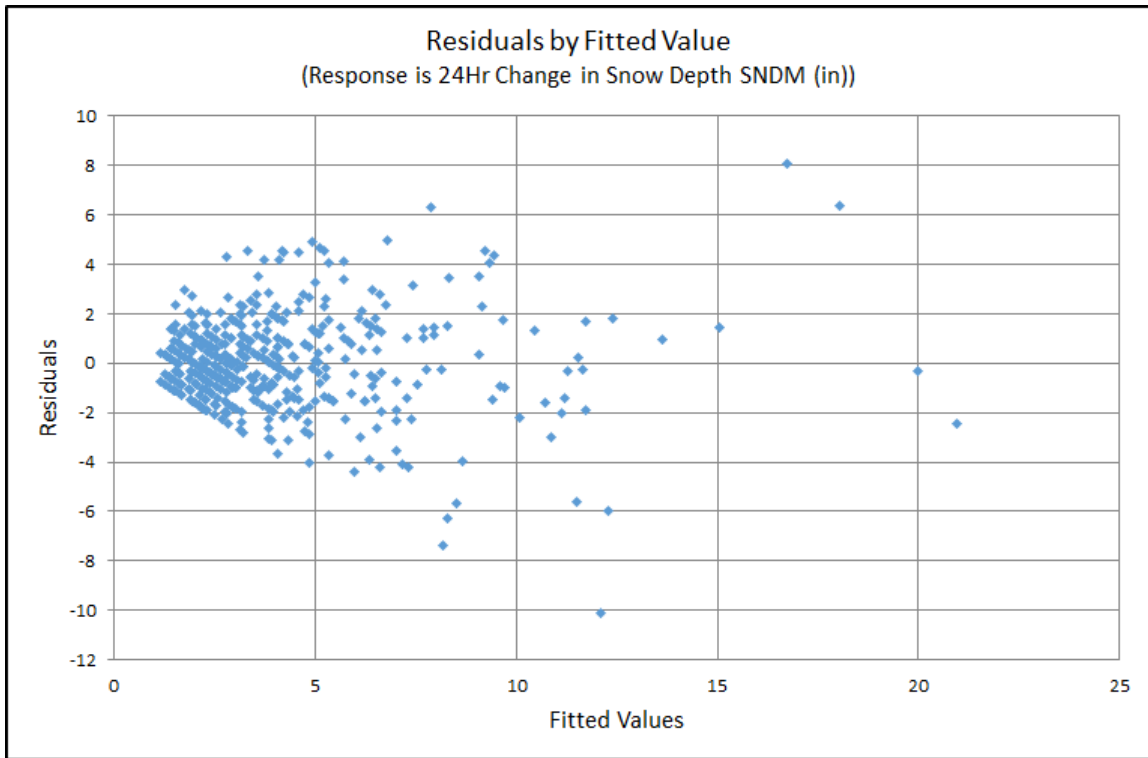


Figure 2. Plot of the residuals by the fitted values for Figure 1.

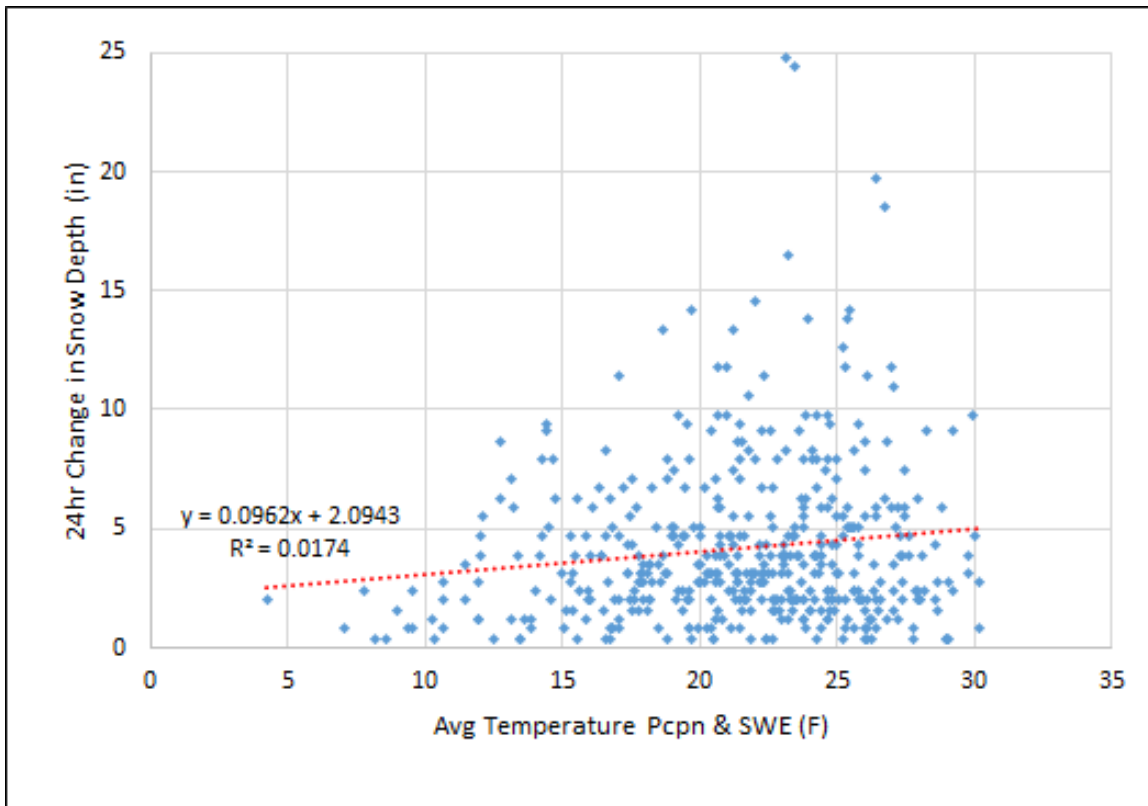


Figure 3. Average Temperature during the period in which Pcpn & SWE were recorded versus the 24-hour Change in Snow Depth. $r^2=0.017$, Adjusted $r^2=0.015$, $S=3.373$, $p\text{-value}=0.0047$.

(22-26°F). Examining the terrain surrounding the Kühtai observation site, there are several mountain ranges towering to 2835-2987 m (9300-9800 ft) MSL which is roughly 980 m (3215 ft) above the site elevation. Using the ridgetop (approximately 2895 m (9500 ft) MSL) as a proxy for winter-time cloud base and an additional 1220 m (4000 ft) for subjective average winter-time cloud depth and a moist adiabatic lapse rate of $-4^{\circ}\text{C}/\text{km}$ ($-3.3^{\circ}\text{F}/1000\text{ ft}$) during snowfall events (Alcott and Steenburgh 2010), one might expect to see cloud temperatures that range from -9.2°C to -18.8°C (15.4°F to -1.8°F) which loosely corresponds to the maximum dendritic growth zone (-12°C to -18°C (10°F to 0°F)) reported by Fukuta and Takahashi (1999). In turn, the maximum dendritic growth zone is known for the production of high snowfall rates and high snow-to-liquid water ratio dendritic snowfalls (Cobb and Waldstreicher 2005), possibly explaining the observed peak in the graph.

Secondly, for any particular temperature value selected in Figure 3, a strikingly wide range of 24hr change in snow depth (SNDM) values are possible which appears to be primarily the result of the water equivalent precipitation associated with each of the individual observation points. To get a truer sense of the impact of temperature on SNDM, we would need to account for the complex interaction effects associated with the water equivalent precipitation. Aggregating the water equivalent precipitation values into subjective incremental groupings and redisplaying those groupings in a color-coded format (Fig. 4), one can see a fairly coarse relationship emerge.

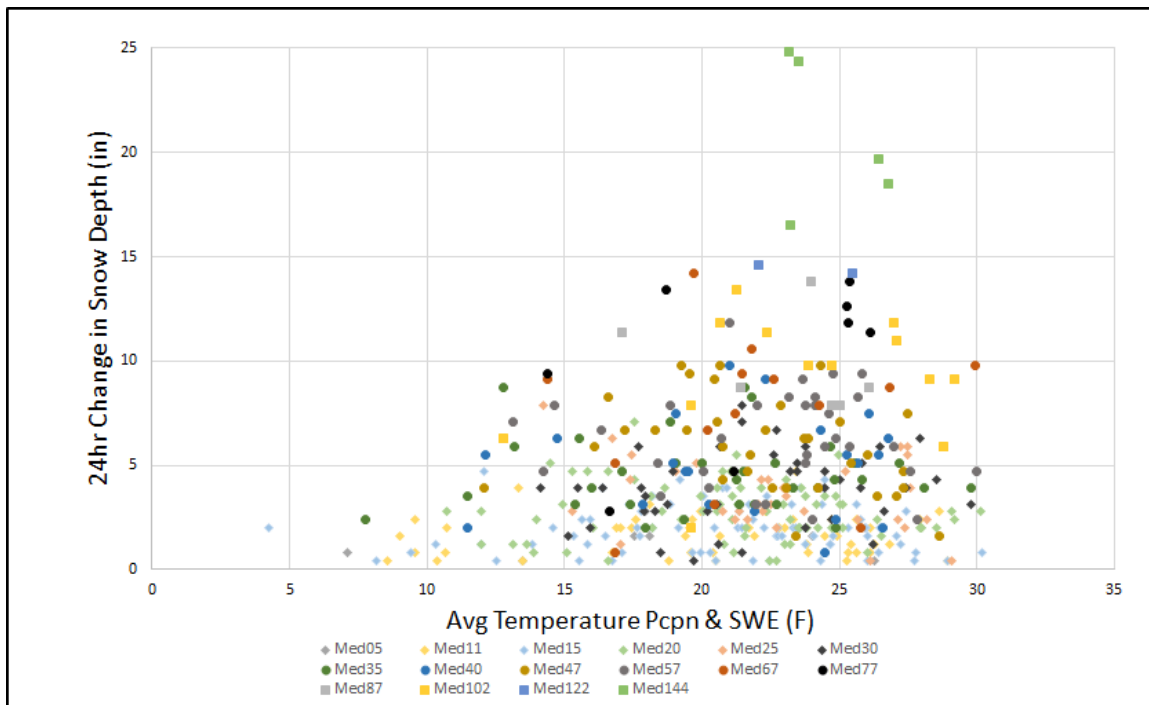


Figure 4. As in Fig. 3, except Average Temperature values are coded (icon and color) based on progressively larger aggregated groupings of Water Equivalent Precipitation.

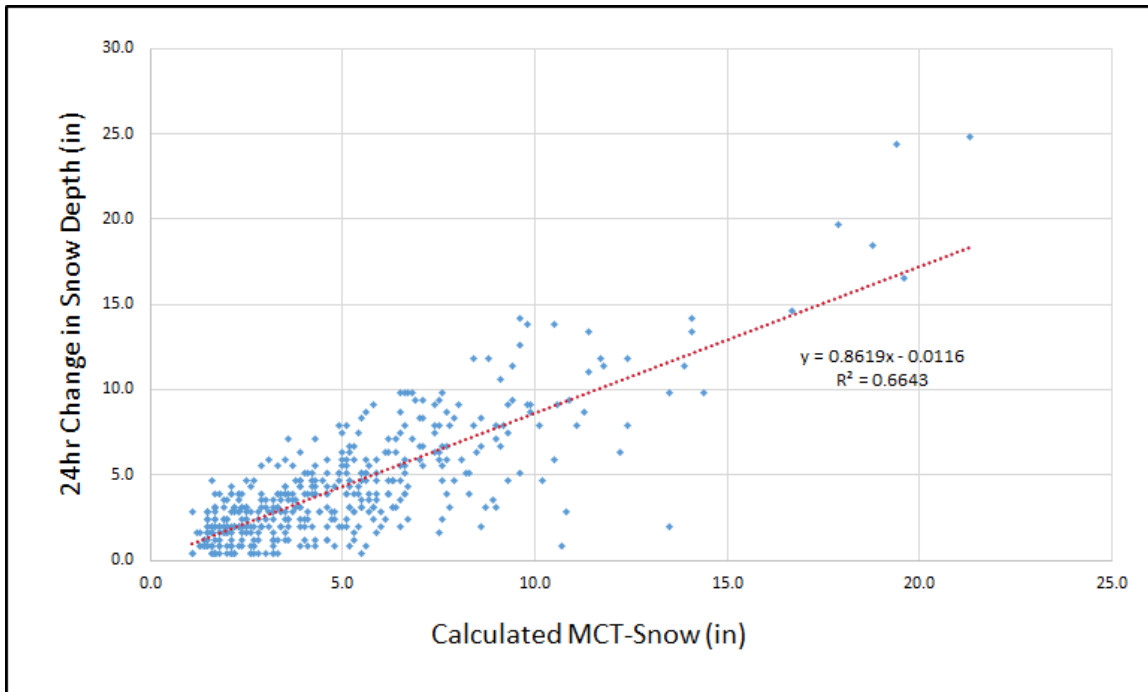


Figure 5. Calculated Snow from the MCT using the Average of Pcpn and SWE and the Average Temperature during Pcpn events versus the 24-hour Change in Snow Depth. $r^2=0.664$, $\text{Adj } r^2=0.664$, $S=1.972$, and $p\text{-value}=1.1\text{E}-109$

One other correlation that was found to be of interest was the relationship between the estimated snowfall using the original MCT and the observed SNDM values as shown in Figure 5. A modest goodness-of-fit ($r^2=0.664$) was depicted while the MCT values consistently over predicted snowfall (a bias effect) when compared to the observed SNDM amounts, which was a point cited in previous research by Roebber et al. (2003) and Alcott and Steenburgh (2010), among a number of other researchers.

B. Redevelopment of the MCT Relationship

Roebber et al. (2003) reported that the original MCT was developed as a quality control aide at the National Center for Environmental Information (NCEI) without providing any further documentation or insight on how it was created. The following methodology, although rudimentary and subjective in nature, was expedient and provided fairly useful results. Utilizing the culled and optimized (or "Best") data set described in Section 2 above, a sample was drawn which included records where the average temperature during the precipitation event was 2.0°C (35.6°F) or colder with measurable water equivalent precipitation ($\text{Pcpn} > 0.0 \text{ mm}$) and snowfall (SNDM or $\text{SND} > 0.0 \text{ cm}$). The data were then iteratively sorted and regrouped in an attempt to reproduce the temperature and water equivalent associations found in the original MCT. First, the data were sorted from highest average temperature to lowest and then subjectively aggregated into 1.7°C (3.0°F) temperature ranges. Each of these temperature-aggregated subdivisions were then further sorted from lowest Average Pcpn & SWE to highest. Finally, in an effort to ascertain the optimal temperature-meltwater-snowfall relationship, the Average Pcpn & SWE and

associated snowfall data falling within a subjective range of meltwater values were gathered within each of the temperature subdivisions so as to adequately populate a Box and Whisker plot from which the median snowfall value was culled for each temperature-meltwater aggregation (e.g., Figure 6). The median temperature, meltwater, and snowfall values gathered from a series of similar such plots were then used to produce temperature-meltwater curves for the various snowfall values (see Figure 7).

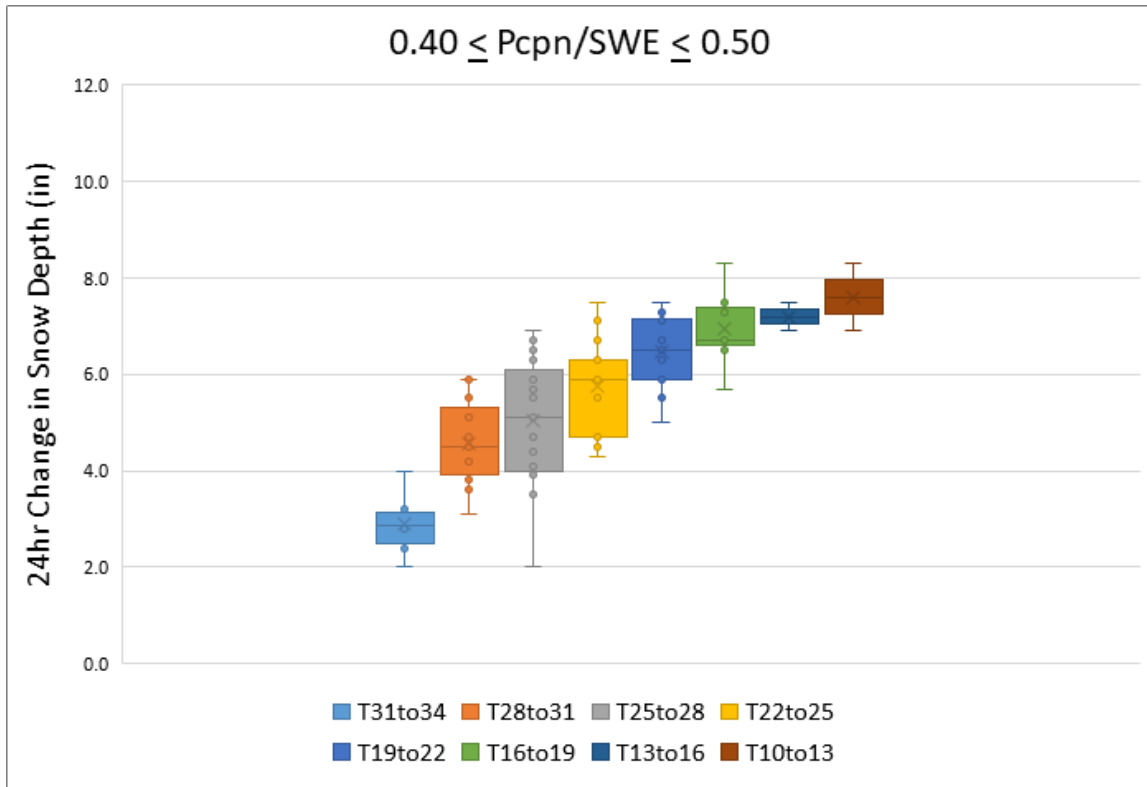


Figure 6. Box and Whisker Plot of the 24-hour Change in Snow Depth (SNDM) for select 1.7°C (3.0°F) temperature intervals (e.g. T31to34) with an Average Pcpn & SWE (meltwater) value falling between 10.1 and 12.7 mm (0.40 and 0.50 in), inclusive.

These meltwater-temperature curves were then utilized as the starting point for further subjective development. Clearly, the Box and Whisker exercise did not eliminate all questionable data as revealed in the MW80 (yellow) and the MW120 (blue) curves which exhibited a visible lack of consistency when compared to nearby curves. Also, due to the limited size of the sample set, the optimum range of use for the curves was limited to temperature values falling between -11.7 and 1.7°C (11 and 35°F) and water equivalent values of approximately 25.4 mm (1.0 in) or less. The following observations and rationale were used to make subjective adjustments to the curves and to extend them beyond these optimal bounds:

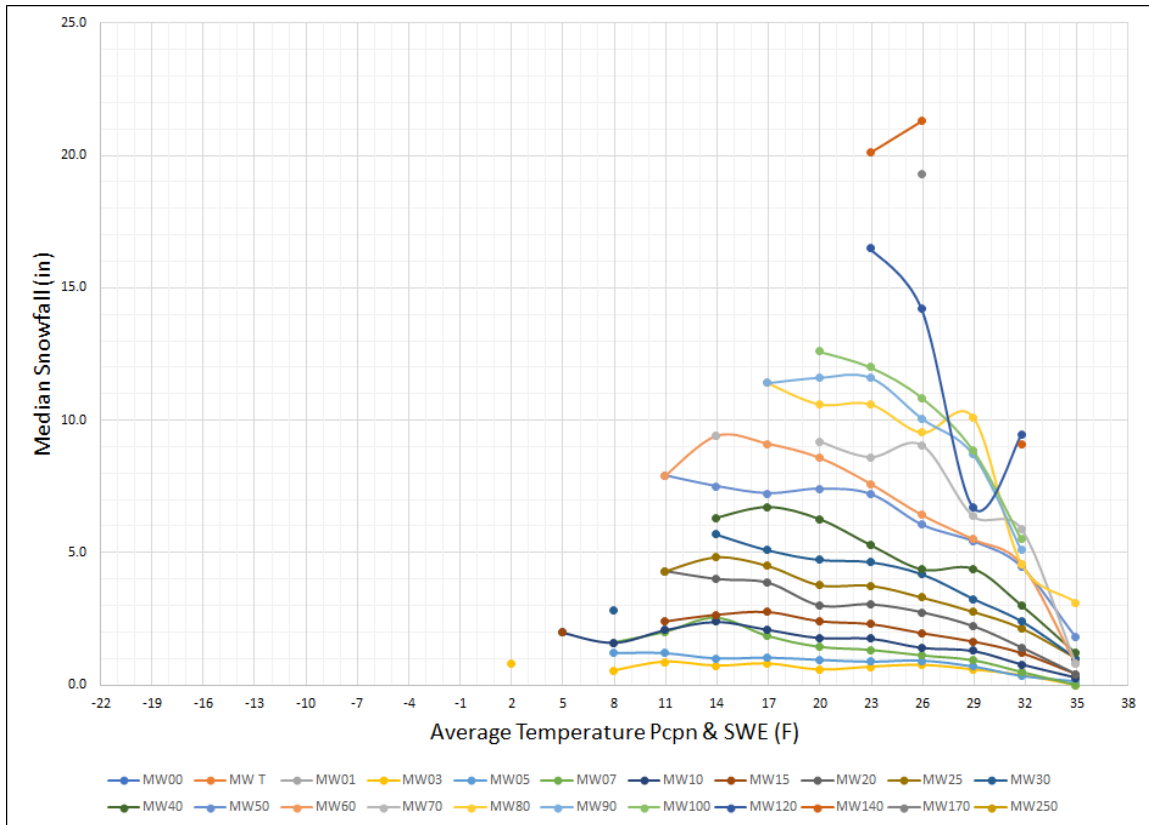


Figure 7. Standard line plots of Median Snowfall (in) versus Average Temperature ($^{\circ}$ F) during precipitation events for subjectively defined water equivalent precipitation (or meltwater) ranges with median values varying from 0.8 to 43.2 mm (0.03 in (MW03) to 1.70 in (MW170)).

1. It appeared that the arc on the preponderance of the curves (MW90 and lower) at the warm end of the spectrum, if extrapolated beyond 1.7° C (35° F) using the slope given by the values between 0 and 1.7° C (32 and 35° F), would terminate at 0.0 cm (0.0 in) of snowfall somewhere between 1.7 and 3.3° C (35 and 38° F). Outside of convective or rapidly accumulating snowfall events, 3.3° C (38° F) appeared to be a reasonable termination point (at least for the current work) for accumulating snowfall.
2. With the exception of several conspicuous points and arcs, the arc on each successively larger meltwater-temperature curve appeared to follow a progressively amplified and concave downward trace. Identifying those arcs with the most reliable curves and/or curve segments and leveraging that information to “inform” the less reliable or truncated curve segments might prove useful in extending the curves, especially in sparse data regions and/or at the extremes of the observational data set.
3. The arc on the preponderance of the curves (MW90 and lower) at the colder end of the spectrum terminates between -13.3 and -10.0° C (8 and 14° F). Operational experience and research (Fukuta and Takahashi 1999) might suggest that snowfall accumulations would likely remain steady or gradually fade

with colder temperatures due to the change in ice crystal habit toward smaller plates.

Given these assertions and subsequent subjective adjustments, the following temperature-meltwater curves (Fig. 8) were constructed. Figure 9 shows the best case scenario where the new temperature-meltwater curves are applied to the “Best” coupled temperature, snow depth, and SWE-Pcpn values in each record to produce an estimated snowfall value. To be clear, utilizing the optimizing process minimizes the interelemental integrity issues identified previously and provides an indication of what might be expected from the temperature-meltwater curves under ideal and perhaps unrealistic automated observational data quality conditions. Besides the very promising correlation values ($r^2=0.975$ for the Standard and Melting categories combined), we see a nearly one-to-one relationship that is no longer biased towards exaggerated estimated snowfall values as was observed with the original MCT table (as seen in Fig. 5). Independent tests of these curves are shown in Section 4.

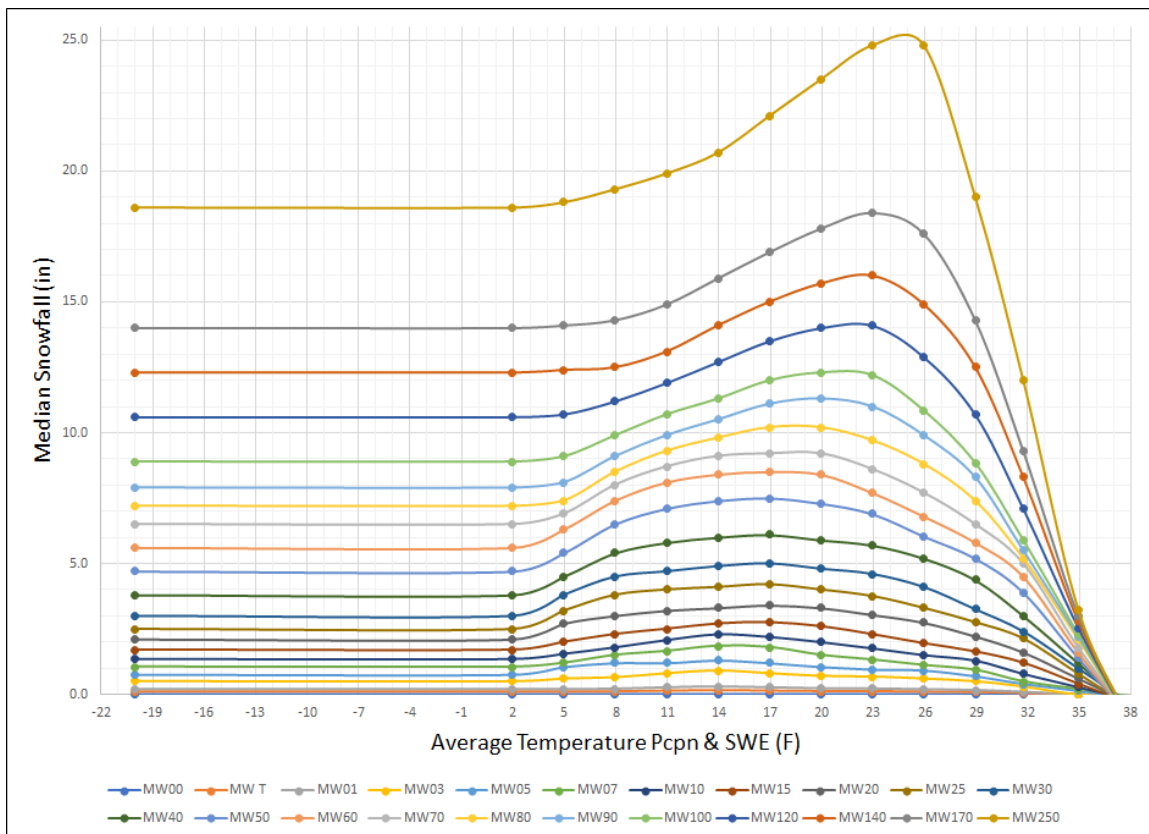


Figure 8. Same as Fig. 7, except subjectively modified and extended as enumerated in the text discussion.

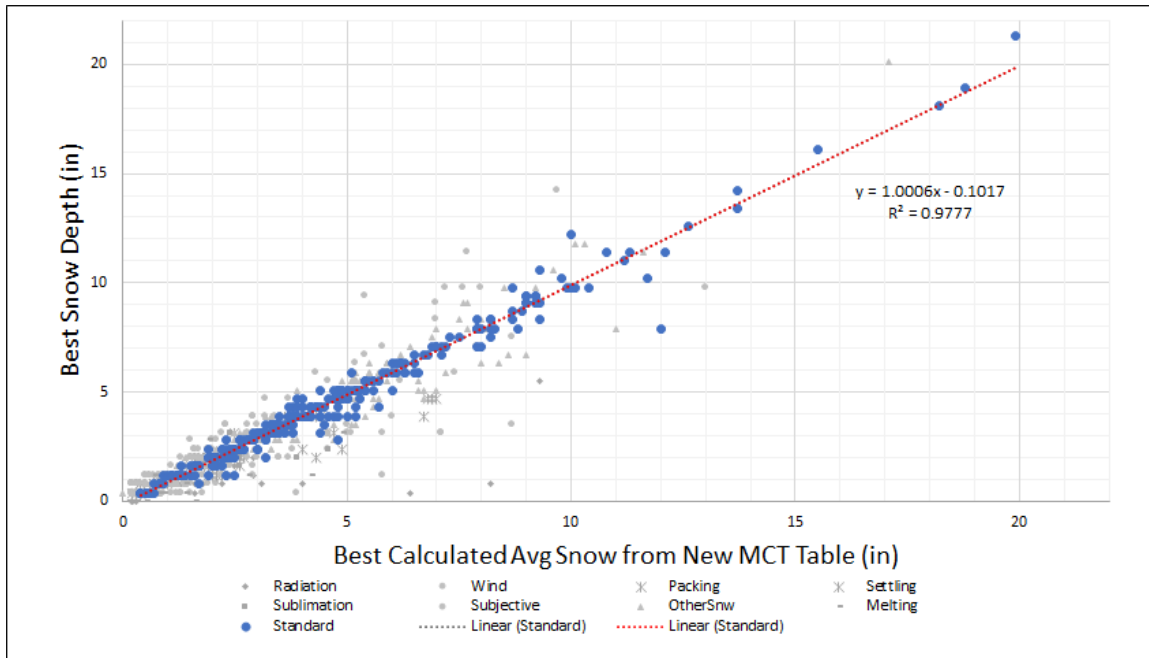


Figure 9. Calculated Snowfall from the Temperature-Meltwater Curves (Fig. 8) using the Best Water Equivalent and Average Temperature during observed Pcpn values versus the Best 24-hour Change in Snow Depth (SNDM or SND). $r^2=0.909$, $Adj\ r^2=0.909$, $S=0.849$, and $p\text{-value}=0.000$ for all data and $r^2=0.975$, $Adj\ r^2=0.975$, $S=0.499$, and $p\text{-value}=3.8E-285$ for Standard and Melting data categories only. Inset of $r^2=0.978$ is for the Standard data category only.

C. OLS Model Development

The preliminary survey results (Section 3.A above) suggested that the main effects (most relevant correlations) associated with snowfall were the total water equivalent precipitation observed and the average temperature observed during the precipitating event. In addition, complicating factors associated with heteroscedasticity and potential interaction effects needed to be considered and/or resolved. The culled and optimized (or “Best”) data set described in section 2 was used to develop the OLS model in further detail in the following sections.

1. Main Effects

a. Meltwater

Here we see a robust correlation (Fig. 10) with Best Meltwater accounting for over 76% of the variance observed in the Best Snow Depth with a standard error (S) just under 1.54 in (3.91 cm). Once again, we see a fan-shape in the residuals (Fig. 11) indicating a problem with heteroscedasticity (Frost 2019).

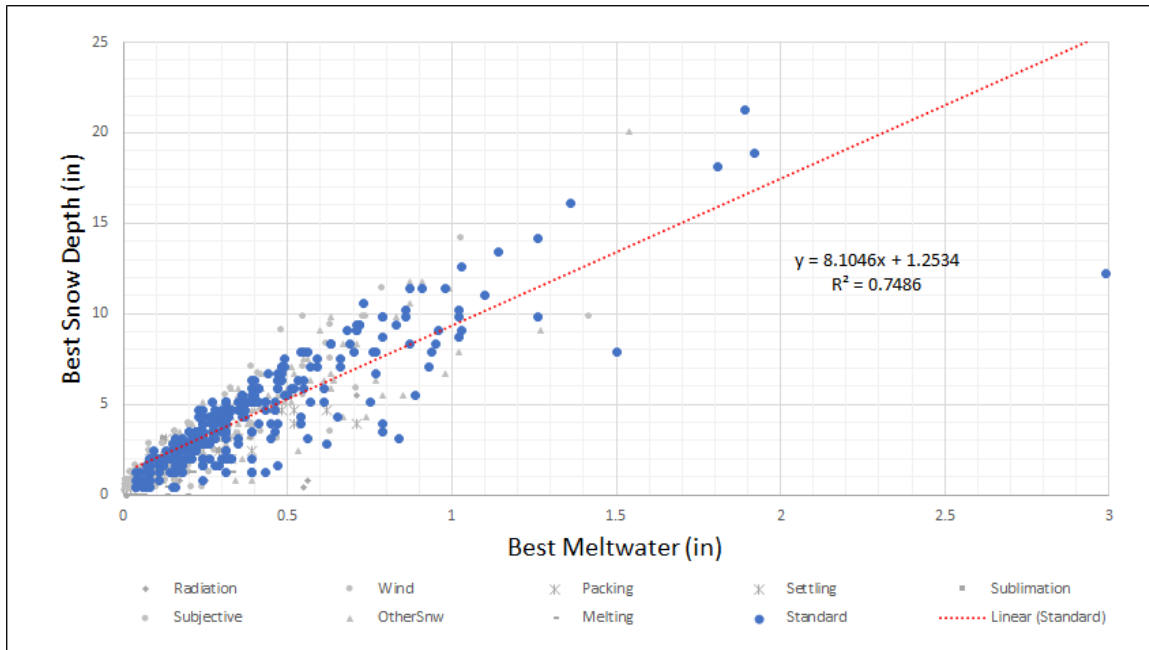


Figure 10. Best Meltwater vs the Best Snow Depth. $r^2=0.762$, Adjusted $r^2=0.761$, Standard Error (S)=1.5355, and p-value=3.1E-112 for the Standard and Melting data set. Inset is for Standard data set only.

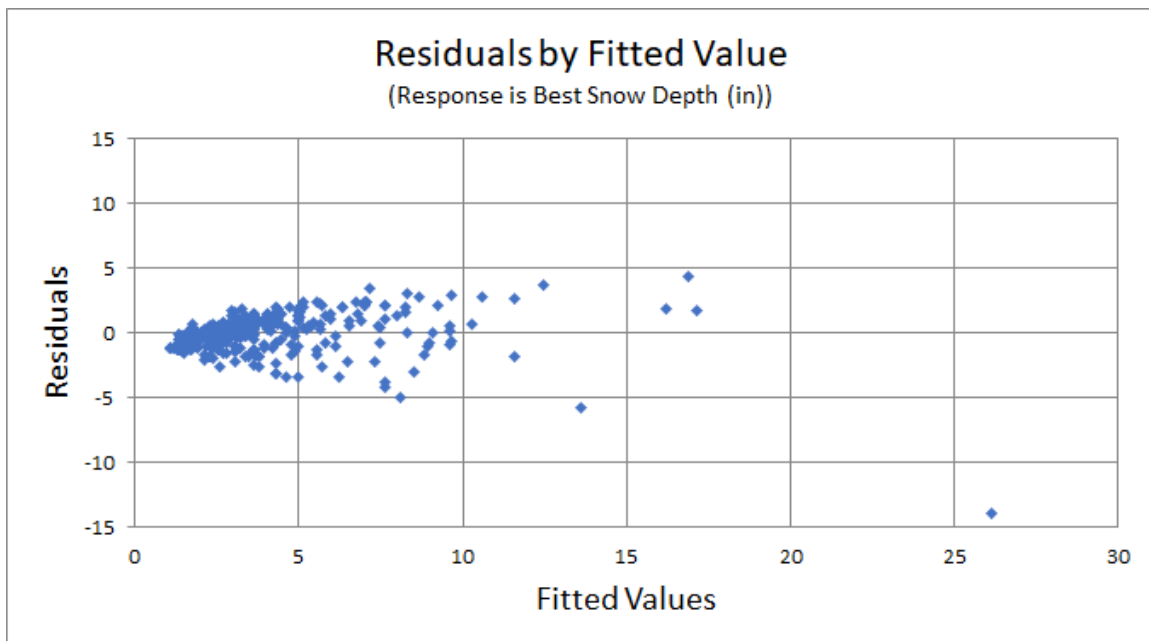


Figure 11. Plot of the residuals by the fitted values for Figure 10.

b. Average Temperature

As was previously discussed in Section 3.A, the correlation between temperature and snowfall is not readily discernible until you consider the interaction effect with meltwater. If you consider the underlying interaction between temperature (AvgT), meltwater (MW), and snowfall, an identifiable relationship becomes more apparent as highlighted in Figure

12. Each of these individual temperature-meltwater relationships are represented fairly well by a second order polynomial (quadratic equation) and will be explored further in Section 3.C.2.b where we deal with Interaction Effects.

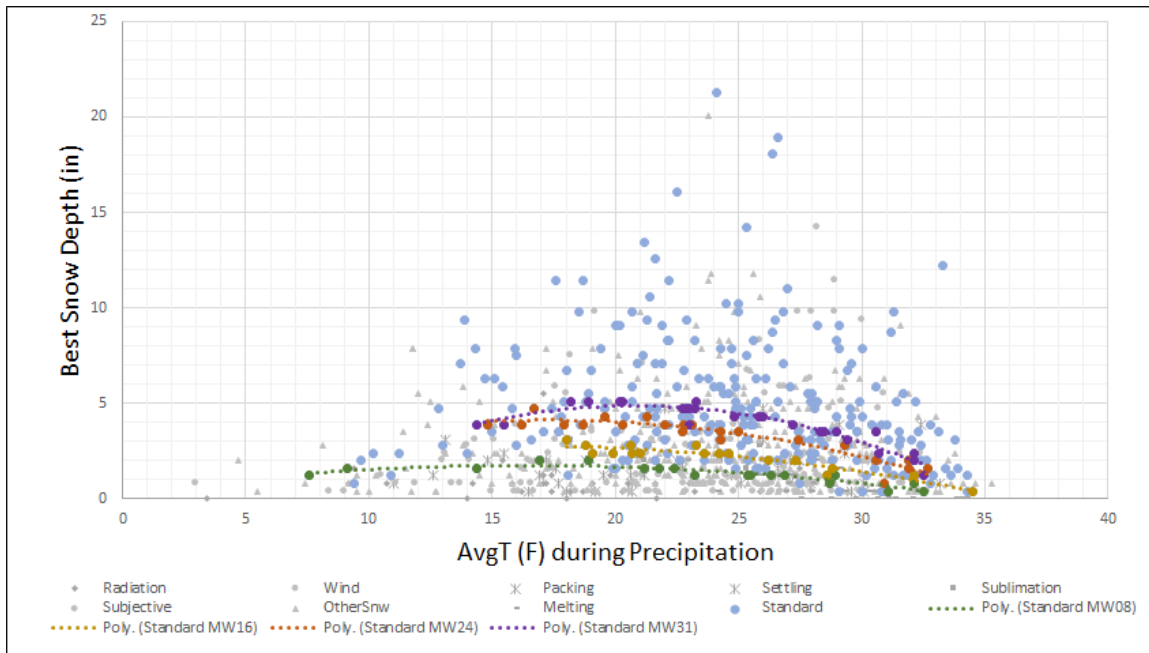


Figure 12. AvgT vs the Best Snow Depth with various meltwater (MW) values color coded (e.g., 0.08 in (green), 0.16 in (gold), 0.24 in (orange), and 0.31 in (purple)) along with the corresponding 2nd order polynomial (quadratic) curve fitting the data values (e.g., Poly. (Standard MW08) for meltwater values of 0.08 in).

2. Special Considerations

a. Heteroscedasticity

There are two types of heteroscedasticity - impure and pure (Frost 2019 here and following). Impure heteroscedasticity refers to cases where you incorrectly specify the model by leaving out one or more important variables which are then absorbed into the error term of the regression equation. If the effect of the omitted variable(s) varies throughout the observed range of data, it can produce telltale signs of heteroscedasticity in the residual plots. Pure heteroscedasticity refers to cases where you specify the correct model and yet you observe non-constant variance in the residual plots. This occurs most often in data sets that have a large range between the smallest and largest observed values and/or are not normally distributed. In the present case, all of these issues are likely occurring as the dependent variable (Best Snow Depth) and independent variable (Best Meltwater) both span two orders of magnitude and are not normally distributed (not shown), and we have yet to test a model that contains all of the identified variables. There are a number of methods that are commonly used to correct cases of pure heteroscedasticity such as redefining the variables, weighted regression, and/or transforming the variable(s). Finding the right fit is to some extent an iterative process of

adjusting the variables, fitting the model, and checking the residuals until the desired effect is achieved (Frost 2019 and PennState 2021). In the interest of brevity, the square root transformation of the meltwater and snowfall variables was found to provide the best resolution for the heteroscedasticity issue. As a result, these variables were used in further development of the OLS model as demonstrated below.

b. Temperature and Meltwater Interaction Effects

Figure 13 is a three-dimensional enhancement of the temperature and meltwater interaction presented earlier in Figure 12. Here we get a much clearer visual sense of the complex interaction between temperature and meltwater, and their combined impact on snowfall. As was noted previously, a 2nd order polynomial (quadratic) curve appeared to capture this effect adequately and was used in further development of the OLS model.

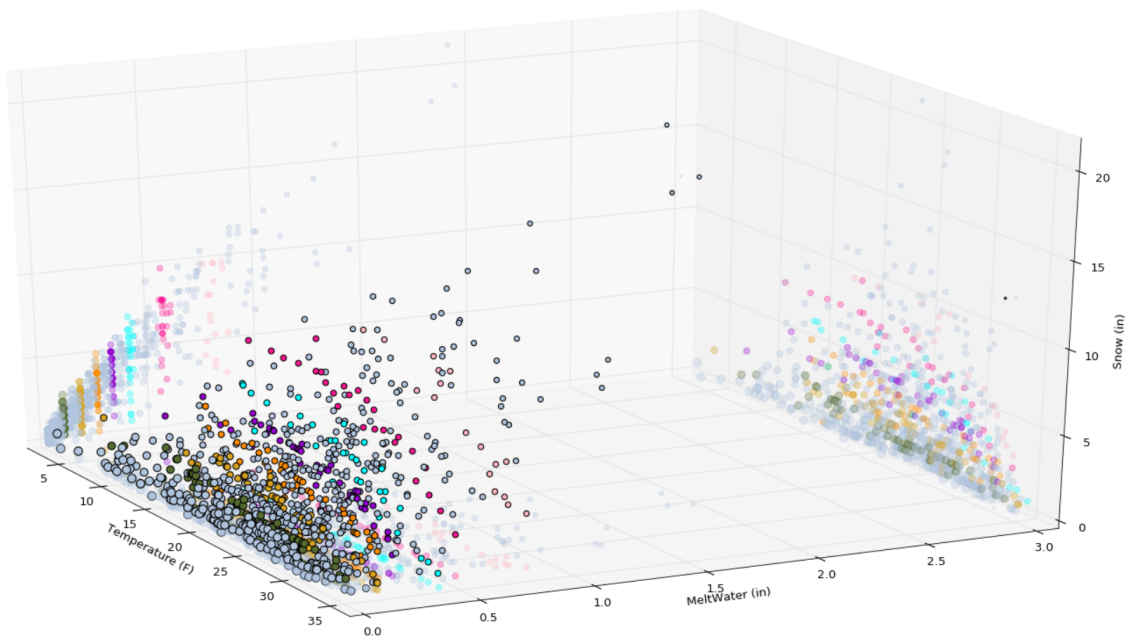


Figure 13. Three-dimensional plot of Temperature (AvgT, °F) vs Best Meltwater (in) vs Best Snowfall (in) for the Standard data set. Various meltwater values have been color coded: 2.03 mm (0.08 in) (green), 4.06 mm (0.16 in) (gold), 6.1 mm (0.24 in) (orange), 7.9 mm (0.31 in) (purple), 9.7 mm (0.38 in) < meltwater < 10.7 mm (0.42 in) (cyan), 13.2 mm (0.52 in) < meltwater < 15.2 mm (0.60 in) (dark pink), and 18.5 mm (0.73 in) < meltwater < 21.8 mm (0.86 in) (salmon). Vibrant colors in the foreground represent the actual data points while the semi-translucent colors are projected as a shadow on the various axes to help visualize the three-dimensional distribution of the data.

3. Results

In an effort to account for the effects of heteroscedasticity and the complex interaction between temperature and meltwater, we performed a multiple regression analysis utilizing the transformed meltwater (Sqrt MW) variable, average temperature (T), the nonlinear quadratic contribution of average temperature (T²), and the interaction between the nonlinear average temperature and transformed meltwater (T²*Sqrt MW) variables as the independent variables and the transformed snowfall (Sqrt Best Snowfall) as the dependent variable. The variables were centered to account for and reduce the multicollinearity effects artificially introduced by the use of the interaction variable (T²*Sqrt MW). Table 1 reflects the statistically significant results that collectively account for over 96 percent of the variance observed in the Sqrt of Best Snowfall.

SUMMARY OUTPUT		Multiple Regression Results on Centered Variables with T ² *MW Interaction						
<i>Regression Statistics</i>								
Multiple R	0.9824454							
R Square	0.965199							
Adjusted R Square	0.9648001							
Standard Error	0.1381624							
Observations	354							
<i>ANOVA</i>								
	<i>df</i>	<i>SS</i>	<i>MS</i>	<i>F</i>	<i>Significance F</i>			
Regression	4	184.7692702	46.19232	2419.858	5.456E-253			
Residual	349	6.662009152	0.019089					
Total	353	191.4312793						
	<i>Coefficients</i>	<i>Standard Error</i>	<i>t Stat</i>	<i>P-value</i>	<i>Lower 95%</i>	<i>Upper 95%</i>	<i>Lower 95.0%</i>	<i>Upper 95.0%</i>
Intercept	1.8692189	0.007343249	254.5493	0	1.85477635	1.883661527	1.854776349	1.883661527
Sqrt MW	3.6459651	0.100323346	36.34214	1.1E-120	3.44865068	3.843279495	3.448650678	3.843279495
T	0.102821	0.009767957	10.52635	1.1E-22	0.08360949	0.122032426	0.083609494	0.122032426
T ²	-0.002572	0.000234047	-10.9888	2.53E-24	-0.0030322	-0.002111584	-0.003032224	-0.00211158
T ² *Sqrt MW	-0.001097	0.00013087	-8.3791	1.32E-15	-0.001354	-0.00083918	-0.001353966	-0.00083918

Table 1. Multiple Regression Results for Sqrt of Best Snowfall vs Sqrt Best Meltwater, AvgT, AvgT², and AvgT²*Sqrt Best Meltwater Interaction. Note the p-values on all the variables are statistically significant.

The resulting OLS snowfall equation is presented below:

$$\text{Snowfall} = [1.8692 + 3.6460(MW^{1/2} - 0.55) + 0.1028(\text{AvgT} - 24.98) - 0.0026(\text{AvgT}^2 - 653.46) - 0.0011(\text{AvgT}^2 * MW^{1/2} - 359.14)]^2,$$

where snowfall and meltwater (MW) are in inches and the average temperature during the precipitation event (AvgT) is in degrees Fahrenheit.

After applying the Snowfall equation above to the Khtai data set, the fitted line plot (Fig. 14), residual plot (Fig. 15), and normal probability plot (Fig. 16) all showed very encouraging results. The fitted line plot showed no bias while the

residual plot appeared to be equally distributed about the zero mean throughout the entire range of fitted values with little or no heteroscedasticity evident.

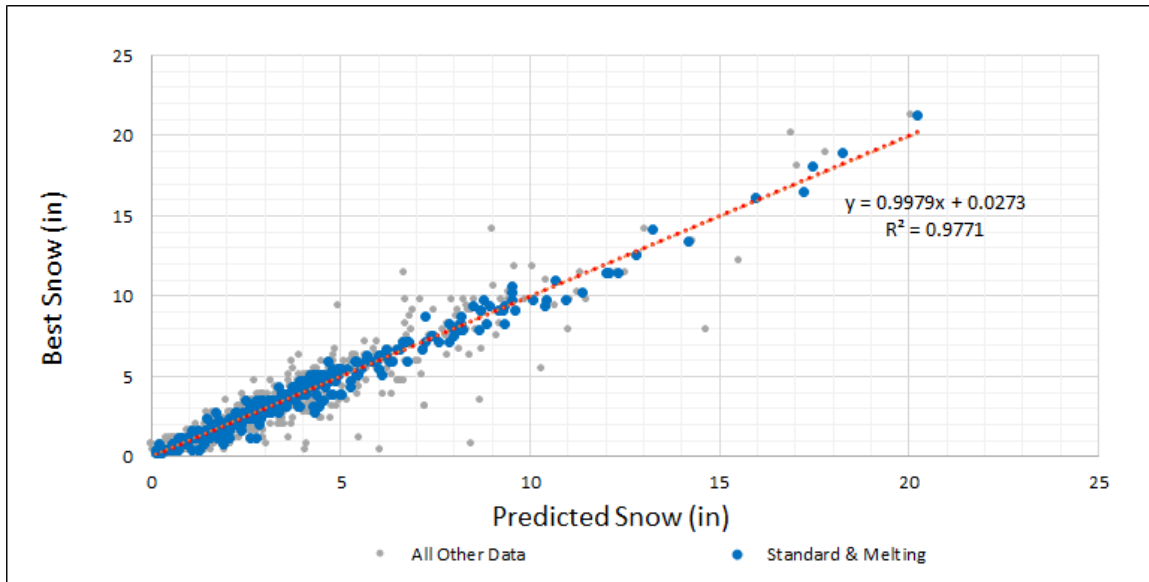


Figure 14. Predicted Snow vs Best Snowfall. Inset for the Standard and Melting data set only.

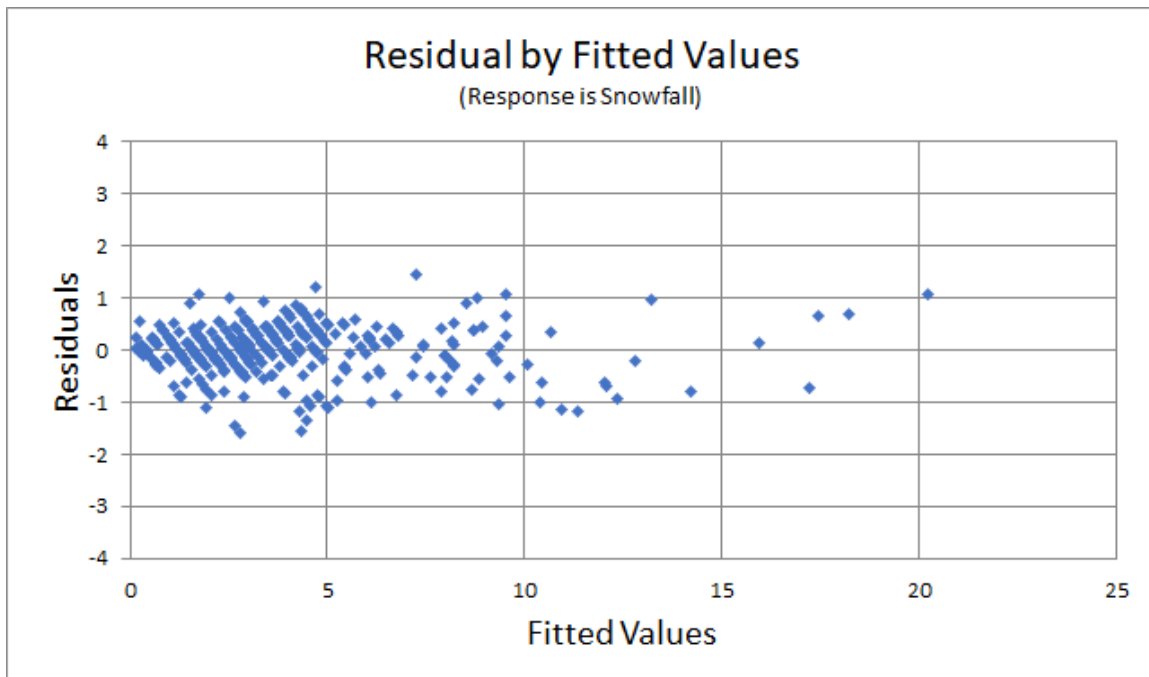


Figure 15. Plot of the residuals by the fitted values for Sqrt Snowfall in Figure 14.

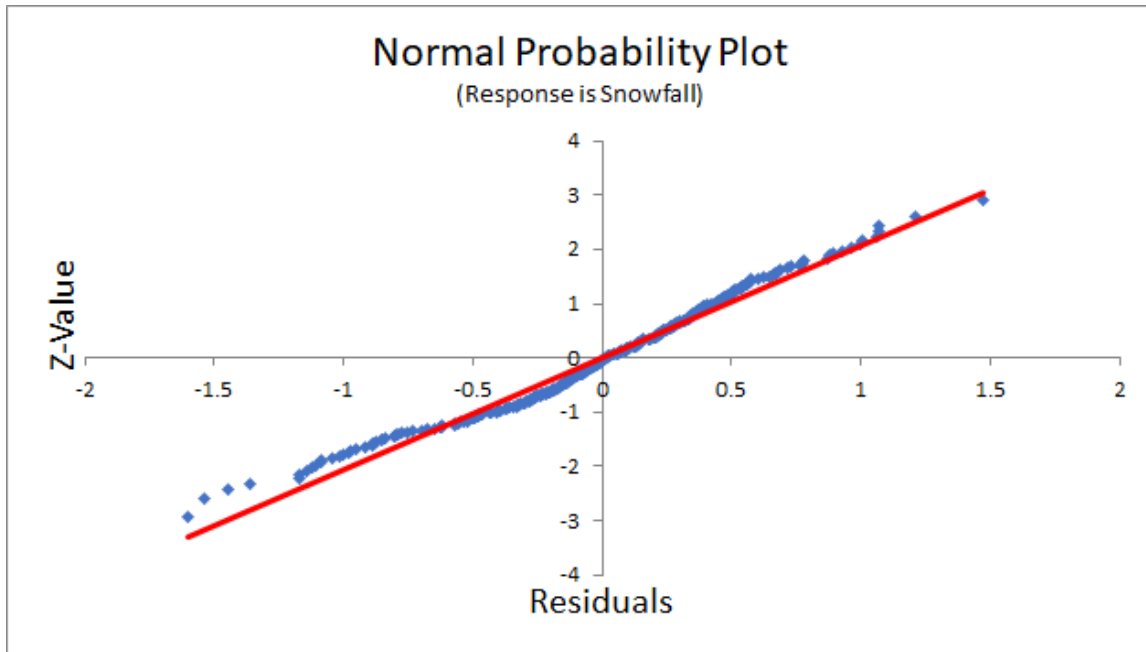


Figure 16. Normal Probability Plot for Best Snowfall in Figure 14.

Upon closer examination of the normal probability plot (Fig. 16), a slight S-shaped curve was evident in the depiction which is typically indicative of shorter than normal tails or insufficient variance (SkyMark 2021). A normality test of the residuals (Georgiev 2021, not shown) confirmed this suspicion both in the failed empirical tests as well as the associated histogram. Based on this evidence, we concluded that the residuals were not normally distributed thus violating one of the optional OLS assumptions (Frost 2019 and 2021). When the residuals fail the normal distribution assumption, it precludes the use of significance levels and significance tests in the verification of the model and in this case the use of the Lower and Upper 95% Confidence Intervals displayed in Table 1.

4. INDEPENDENT TEST RESULTS

Two independent data sets were constructed and used to test the redeveloped MCT curves and OLS results for their suitability in an operational setting. The first data set was constructed from the 6-hourly supplemental snowfall and precipitation climate data captured at the Pocatello Weather Forecast Office since 2013 (hereafter referred to as the Pocatello Data Set). Hourly, 6-hourly, and bulk average temperature, precipitation, and wind data collected from the Automated Surface Observing System (ASOS) located 2.3 km (1.4 mi) northeast of the office were used to augment the 6-hourly supplemental climate measurements. The second data set was constructed from manual snowfall observations taken by the Sun Valley Resort ski operations and augmented by automated observations collected from the Sun Valley Bald Mountain (SVB) SNOTEL site from 2015 through 2020 (hereafter referred to as the Sun Valley Data Set). The SVB SNOTEL site was located in an exposed area near the top of Bald Mountain (43.6612° lat, -114.40315° lon) 3.9 km (2.4 mi) southwest of Ketchum at an elevation of 2747 m (9013 ft) MSL and the ski operations manual observation site was located in a wind-sheltered area northwest

of the SVB SNOTEL site approximately 188 m (617 ft) at an elevation of 2700 m (8860 ft) MSL. The manual snowfall observations were collected each morning at 0600 LT. Automated 15-min observations of temperature, relative humidity, precipitation accumulation, snow depth from an acoustic sounder, and wind speed, direction, and gusts were collected from the SVB SNOTEL site. These data were consolidated and processed into a daily summary record ending at 0600 LT in exactly the same manner as the Kühtai automated data set.

A. Redeveloped MCT Results

1. Pocatello Data Set

Snow days from 2015 to 2020 where the maximum temperature (T_{max}) was 3.3°C (38°F) or less and the sum of the hourly wind observations (W_{tot}) for the day fell below 89.8 m/s (201 mph) were utilized in conjunction with the redeveloped MCT curves (Fig. 8) to calculate daily snowfall accumulations from hourly (Fig. 17), 6-hourly (Fig. 18), and bulk (Fig. 19) time-scale renderings to examine the corresponding results.

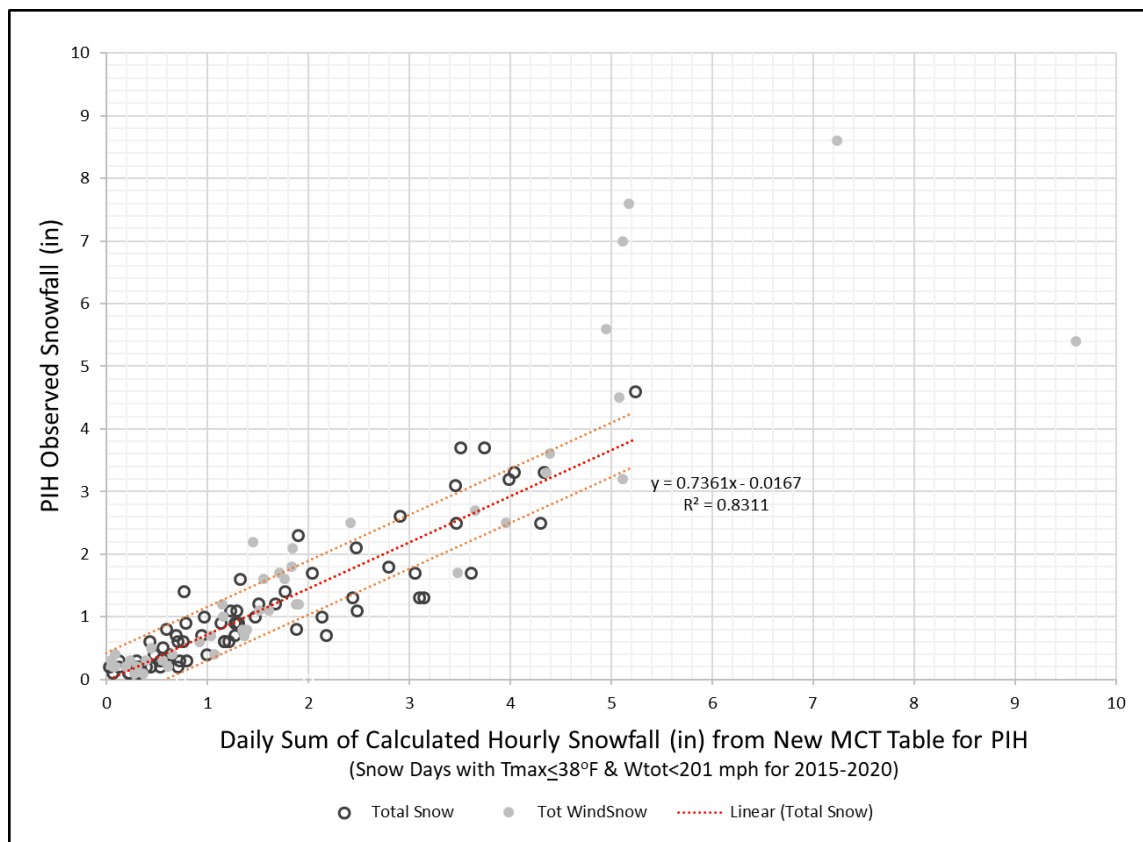


Figure 17. Daily sum of hourly snowfall estimates calculated using the redeveloped MCT curves (or New MCT Table) for snow days with $T_{max} \leq 3.3^{\circ}\text{C}$ (38°F) and $W_{tot} < 89.8\text{ m/s}$ (201 mph) at Pocatello (PIH) from 2015-2020. $r^2=0.8311$ (inset), $\text{Adj } r^2=0.8287$, $S=0.4275$, and $p\text{-value}=9.67\text{E-}29$. The red line represents the best fit regression line and the orange lines represent the standard error (S). Circled values (o) represent the daily total hourly snowfall estimates.

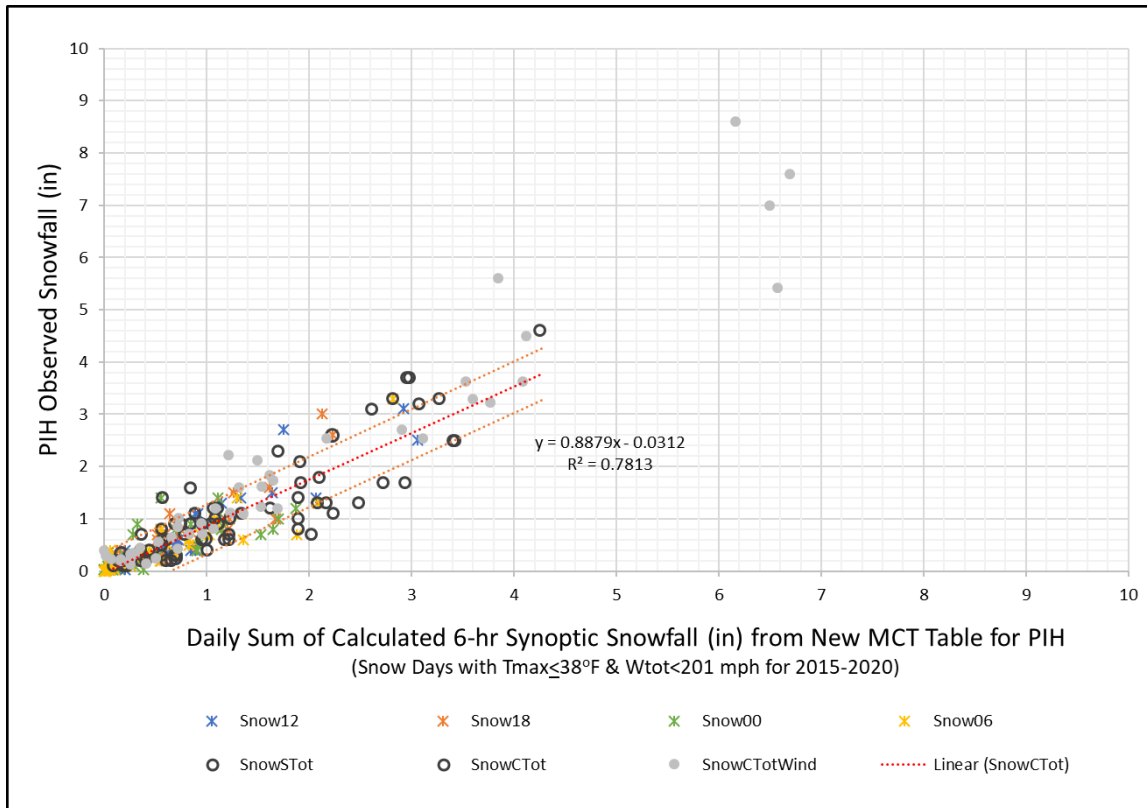


Figure 18. Daily sum of 6-hourly snowfall estimates calculated from the redeveloped MCT curves (or New MCT Table) for snow days with $T_{max} \leq 3.3^\circ\text{C}$ (38°F) and $W_{tot} < 89.8$ m/s (201 mph) at Pocatello (PIH) from 2015-2020. $r^2=0.7813$ (inset), $\text{Adj } r^2=0.7781$, $S=0.4806$, and $p\text{-value}=3.90\text{E-}24$. The red line represents the best fit regression line and the orange lines represent the standard error (S). Starred values (*) represent the 6-hourly synoptic snowfall subtotals. Circled values (o) represent the daily total 6-hourly snowfall estimates.

Regarding the daily sum of hourly snowfall estimates (Fig. 17), we see a definite over-forecast bias, improving with the daily sum of the 6-hourly snowfall estimates (Fig. 18), and ending with no forecast bias indicated in the bulk snowfall rendering (Fig. 19). Also of interest here is the increased scatter observed when moving from the hourly to the bulk rendering which had a deleterious impact on both the goodness of fit and the standard error statistics for the bulk case. These results likely suggest that the hourly rendering does a good job of capturing the short term snowfall vagaries associated with natural temperature and precipitation variability observed within a storm cycle while failing to account for the densification, overburden, and metamorphosis of the snowpack normally observed during a 24-hour observation period ultimately resulting in the over-forecast bias. The opposite is most likely occurring in the bulk application where much of the dynamic hourly interplay is attenuated resulting in greater scatter while the metamorphosis of the snowpack is “encapsulated” as it were within the model resulting in the non-biased outcome.

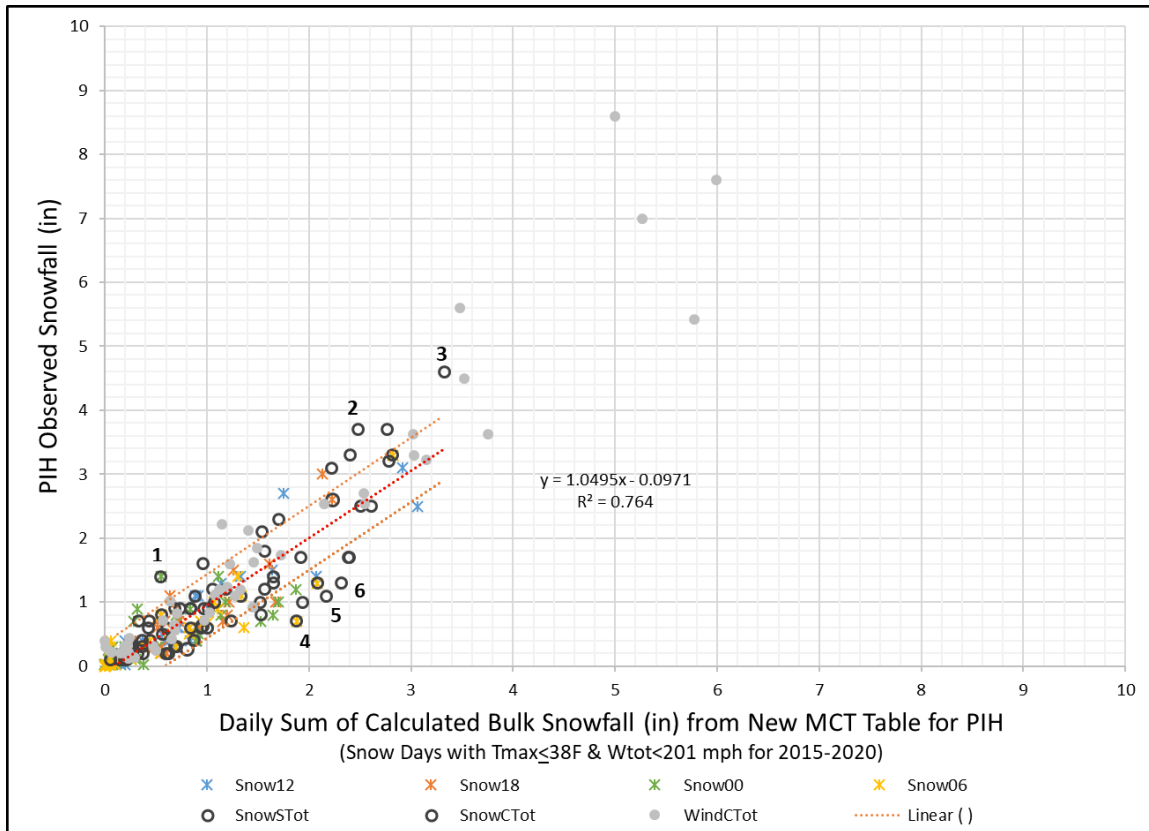


Figure 19. Daily bulk snowfall estimates calculated from the redeveloped MCT curves (or New MCT Table) for snow days with $T_{max} \leq 3.3^{\circ}\text{C}$ (38°F) and $W_{tot} < 89.8$ m/s (201 mph) at Pocatello (PIH) from 2015-2020. $r^2=0.7640$ (inset), $Adj\ r^2=0.7605$, $S=0.4993$, and $p\text{-value}=5.26\text{E-}23$. The red line represents the best fit regression line and the orange lines represent the standard error (S). Starred values (*) represent the 6-hourly synoptic snowfall subtotals. Circled values (o) represent the daily bulk snowfall totals. See text concerning enumerated data points 1-6.

In an effort to test these suppositions, a number of outlying points were identified in the bulk application (see enumerated points in Fig. 19) with a more granular examination of each case provided below. Points 1 through 3 were utilized to examine those cases that were underestimated by the model and points 4 through 6 represented those cases that were overestimated. At sample point 1, the hourly data indicated temperatures rising abruptly from -0.5°C (31°F) at 23:53 UTC to 1.1°C (34°F) at 00:37 UTC after recording 1.27 mm (0.05 in) of precipitation. If the bulk calculation had been done using the average temperature found during the time the “measurable” precipitation was observed (in this case -0.5°C (31°F)), the redeveloped MCT curves suggest that the bulk snowfall estimate would have been 2.8 cm (1.1 in) which would have brought the observed and estimated points into much closer agreement. For point 2, the temperature dropped steadily over the course of several hours from -6.1°C (21°F) to -7.2°C (19°F) with light to moderate precipitation ongoing throughout the entire six-hour event. During the period of heaviest snowfall, sustained wind speeds peaked at 7.6 m/s (17 mph). It was at this time that

a suspicious 6-hourly snowfall observation of 6.9 cm (2.7 in) was recorded. The recorded observation was roughly 2.3 cm (0.9 in) more than anticipated given the temperature and precipitation values recorded during that time frame, raising concern that perhaps either an undercatch of liquid was recorded in the precipitation gauge and/or an excess of wind-deposited snow was measured on the snow board. In either case, there appeared to be a notable lack of coherence between the measurements. For point 3, the hourly observations showed a gradual swing in temperatures from -6.1°C (21°F) to -9.4°C (15°F) and back up to -5.0°C (23°F) over the course of a 14-hour period. During this time, the heaviest hourly precipitation occurred when the temperature was at or near -9.4°C (15°F). The bulk average temperature for the entire time frame was -6.7°C (20°F). Regardless of whether -9.4°C (15°F) or -6.7°C (20°F) was used in the calculation, the redeveloped MCT curves showed a similar outcome of 8.4 cm (3.3 in) of total snowfall which remained well below the 11.7 cm (4.6 in) value reported for the day. In this instance, it may have been instructive to review radar imagery and/or the vertical temperature profile to ascertain whether mesoscale enhancements and/or vertical thermal profiles and lift may have played a part in producing conditions conducive to enhanced dendritic snow growth during the observation period. At point 4, 2.0 mm (0.08 in) of precipitation was recorded under light winds and steady temperatures near -7.8°C (18°F). Under these conditions, the redeveloped MCT curves suggested 4.6 cm (1.8 in) of snowfall while the observation indicated a questionable 1.8 cm (0.7 in) snowfall event. Again, it may have been instructive to review the vertical temperature profile for this period to determine the potential crystalline structures of the snowfall before labeling the observation as potentially errant. For point 5, we see an extended period with trace precipitation amounts and temperatures ranging from -8.9°C (16°F) to -7.2°C (19°F) followed by a period with measurable precipitation and warmer temperature readings near -5.6°C (22°F). Here, the longer and colder period with trace amounts of precipitation is equally weighted with the shorter and warmer period with measurable precipitation effectively skewing the bulk average temperature used in the calculation toward a lower value of -7.2°C (19°F) resulting in an elevated snowfall estimate. If -5.6°C (22°F) were used for the bulk average temperature, the resulting estimate of 4.1 cm (1.6 in) would have been much more comparable to the observed 2.8 cm (1.1 in) snowfall. At point 6, we have a period with very cold -13.3°C (8°F) ambient temperatures and precipitation accumulating to 2.3 mm (0.09 in) within a 6-hour period followed by a questionably low snowfall report of 2.0 cm (0.8 in). Under these conditions the redeveloped MCT curves suggest a 5.1 cm (2.0 in) snowfall. Recall that the redeveloped MCT curves were subjectively extended to capture colder events such as this and this case may very well suggest the need to revise the curves lower for these colder events.

2. Sun Valley Data Set

Snow days from 2015 to 2020 where the maximum temperature was 3.3°C (38°F) or less were utilized in conjunction with the redeveloped MCT curves to estimate snowfall for the Sun Valley site. Figure 20 depicts the calculated snowfall for the SVB SNOTEL data versus the manually observed 24-hour snowfall reported by the Sun Valley Resort ski operations staff. The statistical results show a very slight overpredictive bias with a modest correlation accounting for about 87% of the variance ($r^2=0.8743$) in the Observed Snowfall and a standard error of 1.08 in (2.7 cm) for the windy, melting, and standard data sets combined. Here we have included the windy data set in the calculation due to the relatively small number of melting and standard cases available at this wind prone site. By doing so, it is believed that the windy data set likely introduced snowfall data that may have undergone enhanced densification due to fracturing of the snow crystals leading to the slight overprediction bias.

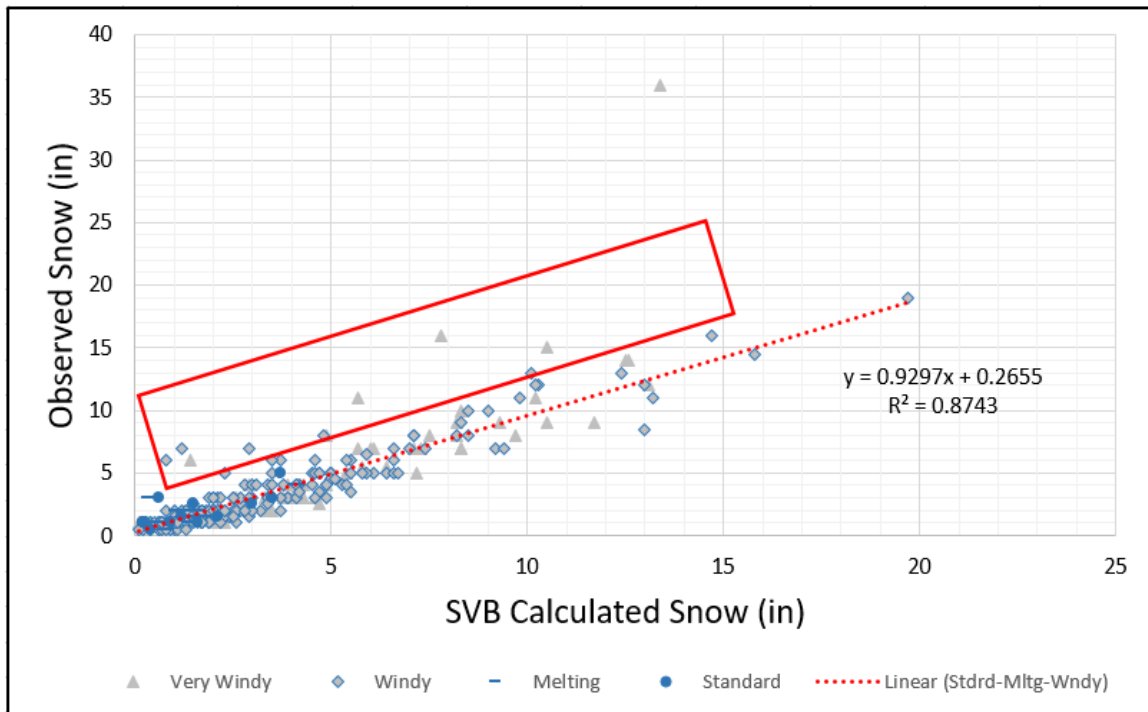


Figure 20. Calculated Snowfall for SVB SNOTEL using the redeveloped MCT curves (or New MCT Table) versus the Observed Snowfall for 2015-2020. $r^2=0.8743$ (inset), $Adj\ r^2=0.8737$, $S=1.077$, and $p\text{-value}=1.2E-104$ for the windy, melting, and standard data. Red rectangle encompassing overperforming data points.

Curiously, there are also a handful of conspicuous underestimated points (see red rectangle Fig. 20) and what appears to be a fairly obvious outlier with a reported 24-hour snowfall of 36 in (91.4 cm). Upon closer inspection of this latter data point, it was confirmed to be at considerable odds with the reported 24-hour change in snow depth of 19.0 in (48.3 cm). As for the underestimated points, some of which are more than double the calculated value, we can only speculate that there may have likely been a significant

undercatch of water equivalent precipitation at the automated SVB gauge and/or difficult snowfall measurement conditions at the manual observation site due to wind. Also, as previously discussed, forced mesoscale terrain and/or vertical temperature profile and lifting mechanisms may have played a part in the enhanced snowfall conditions.

B. OLS Results

1. Pocatello Data Set

Once again, snow days from 2015 to 2020 where the maximum temperature (T_{max}) was 3.3°C (38°F) or less and the sum of the hourly wind observations (W_{tot}) for the day fell below 89.8 m/s (201 mph) were utilized in conjunction with the OLS snowfall equation to calculate a bulk daily snowfall accumulation (Fig. 21). Here we see a modest and unbiased result with nearly 71% of the variance ($r^2=0.7052$) in the Observed Snowfall being accounted for by the OLS snowfall with a standard error of 0.56 in (1.4 cm). The enumerated days identified in figure 19 were similarly labeled in figure 21 for comparison purposes. The OLS results are similar to the redeveloped MCT results but with slightly larger spread resulting in a degraded goodness-of-fit value.

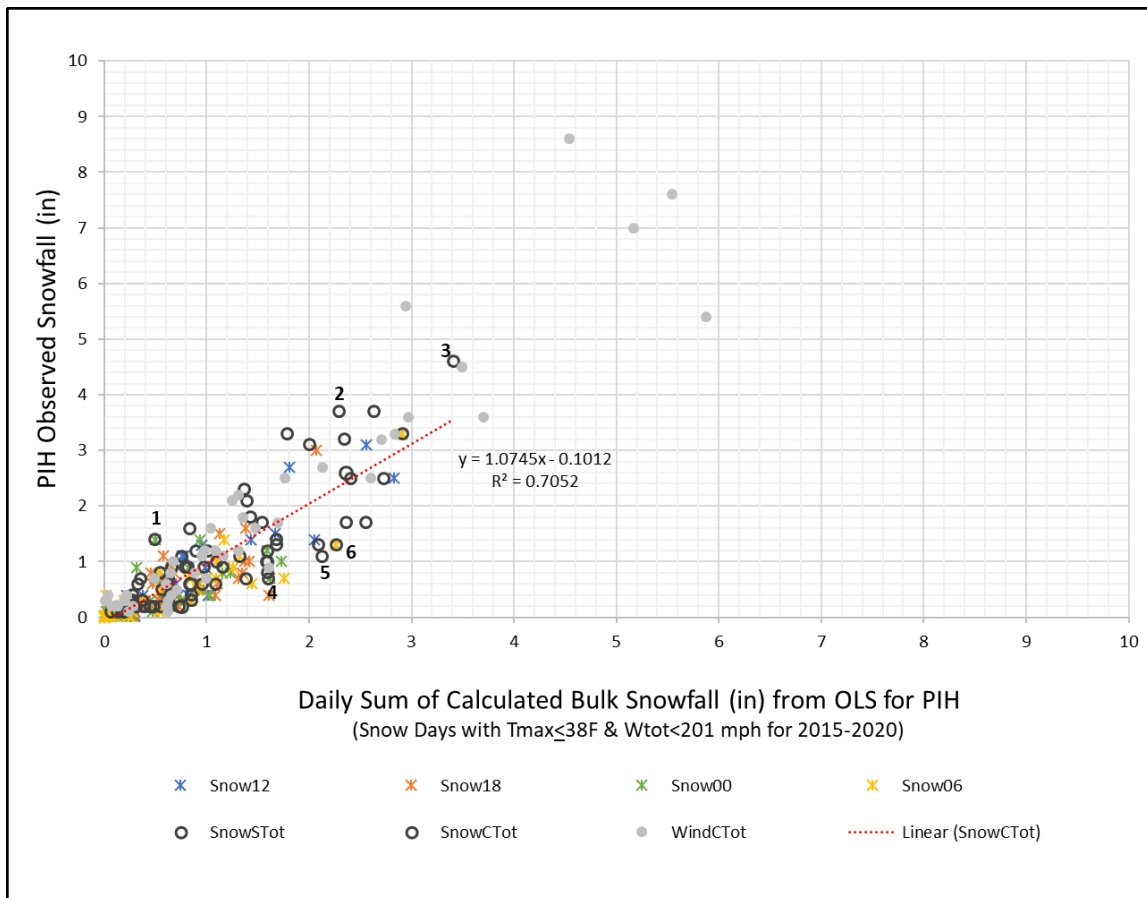


Figure 21. Calculated Snow from the OLS equation for Snow Days with $T_{max} \leq 3.3^{\circ}\text{C}$ (38°F) at Pocatello (PIH) from 2015-2020. $r^2=0.7052$ (inset), Adj $r^2=0.7009$, $S=0.5580$, and $p\text{-value}=1.05\text{E}-19$ for the daily observed snowfall (SnowCTot). Starred values (*) represent the 6-hourly synoptic subtotals.

2. Sun Valley Data Set

Snow days from 2015 to 2020 where the maximum temperature was 3.3°C (38°F) or less were utilized in conjunction with the OLS snowfall equation for the Sun Valley site (Figure 22). Here we see a favorable correlation ($r^2=0.8572$) with a standard error of a little over 1.14 in (2.9 cm) and a slight overprediction bias for the windy, melting, and standard data sets. As was noted previously, the windy data set was added to the calculation to compensate for the relatively small number of melting and standard cases available at this normally windy site. By doing so, it is believed that the windy data set likely introduced a significant portion of data that had undergone destructive crystal alterations primarily due to fracturing which resulted in a densification of the snowfall and hence a slight bias toward overprediction. Once again, a similar number of underestimated windy cases were observed along with one erroneous data point (36 in (91.4 cm) observed value).

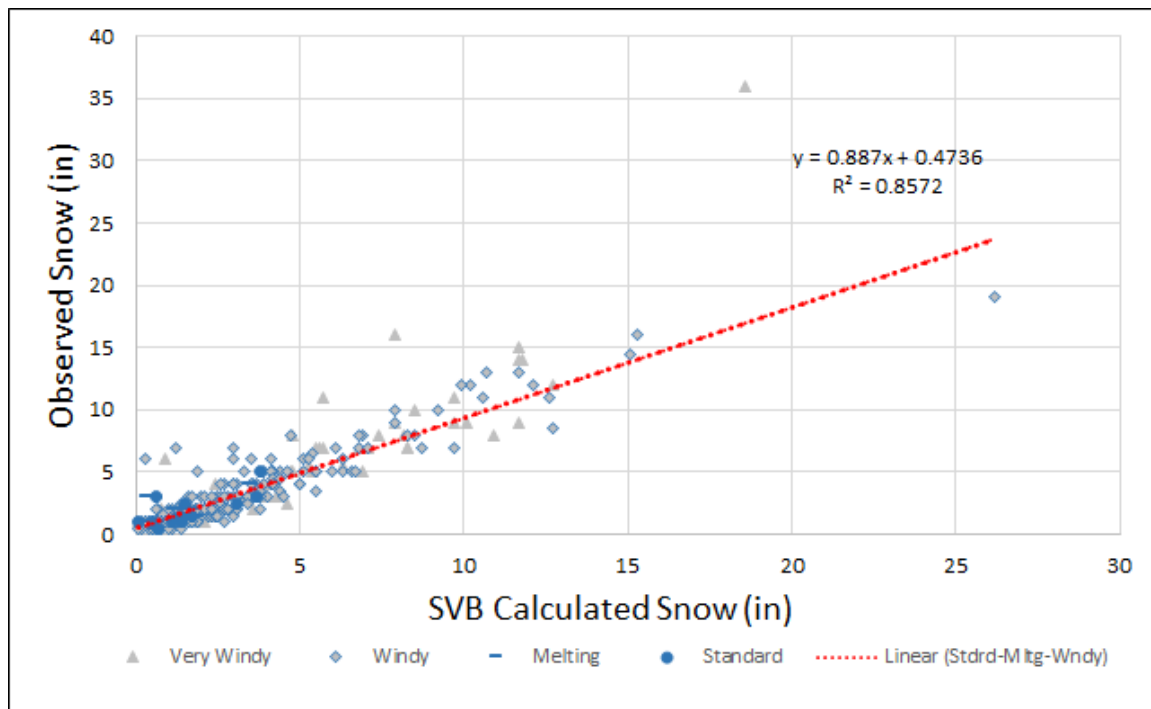


Figure 22. Calculated Snowfall for SVB SNOTEL using the OLS equation versus the Observed Snowfall for 2015-2020. $r^2=0.8572$ (inset), $Adj\ r^2=0.8570$, $S=1.148$, and $p\text{-value}=2.55E-98$ for the Windy, Melting, and Standard data.

5. DISCUSSION AND CONCLUSIONS

In an effort to produce reasonably accurate, timely, and consistent snowfall estimates in an operational setting, two distinct models were developed for use with automated meteorological platforms – a redeveloped version of the widely discarded New Snowfall to Estimated Meltwater Conversion Table (MCT) and a statistical model based on Ordinary Least Squares (OLS) methods. Tests of these models on local independent

data sets (see Section 4) produced encouraging results with no bias as was previously reported with the original MCT. Due to natural limitations associated with the Kùhtai data set, the use of the redeveloped MCT curves and OLS equation would be best applied to snowfall events where temperature values ranged between -11.7 and 1.7°C (11 and 35°F) and 24-hour water equivalent precipitation values fell below 25.4 mm (1.0 in). In an effort to overcome these limitations, future work might test whether “grafting” additional data sets and/or extreme events from colder continental climate regimes onto the Kùhtai data set may help to extend the objective reach of the models. Areas with a strong marine, topographical, and/or frequent organized deep frontogenetic influences (e.g., Sierra or Cascade Mountain Ranges, and Midwest states) may find these results unsuitable for operational use due to differences in climate, thermodynamic, and/or dynamic forcing characteristics unique to those regions. Testing the equations on local data sets may help to alleviate some of these concerns.

The methodology used to produce the redeveloped MCT curves was highly subjective, labor intensive, prone to error and bias, and likely not easily reproducible. Spatial interpolation techniques such as inverse distance weighting, cubic splines, Kriging, and/or nearest neighbor (Hennemuth, B. 2013), among others, might help to improve the results as well as alleviate many of the concerns over the subjective techniques used to develop and extend the curves. These interpolation techniques would have to be suitable for irregularly spaced and discontinuous data samples over 2- and 3-dimensional relational space to be of any use in this application.

A number of instances were highlighted where the observed snowfall varied considerably from the estimated snowfall value. In most of these cases, the corresponding observations proved very helpful in deconstructing the events and exposing errors and inconsistencies rooted in observational practices, and limitations in the modeling effort associated with the constrained data set used during development. Additionally, questions remained as to the possible influence of mesoscale terrain enhancements and/or vertical thermal profiles and lift to enhanced dendritic snow growth and snowfall events. Ongoing work by several researchers in the Midwest (Hultquist 2020; Baumgardt, Schmidt, and Just 2020) have focused on frontal environments favorable for high snow-to-liquid water ratios, and further investigation into this aspect of the current study would be of interest.

Tests of both models on an independent data set showed that the OLS results were slightly weaker in both goodness-of-fit and standard error. One possible reason for this result may have something to do with how well the temperature effects were captured by the quadratic equation used during the development of the statistical model. In the redevelopment of the MCT curves, a cubic spline was used to fit the data more closely and thus, it may prove beneficial to explore the use of other functions to more adequately capture the varying nonlinear temperature aspects of the data. Additionally, it was found that the residuals were not normally distributed in the OLS model which violated one of the optional assumptions and precluded the use of significance levels and significance tests. Initially, it was thought that constraining the data to include only the standard and melting categories may have been too stringent. As was mentioned previously, grafting extreme events and/or colder continental data

sets onto the Kühtai data set in addition to relaxing the above constraints might prove helpful in increasing the variability needed to normalize the residuals.

Both equations were developed using bulk water equivalent precipitation values obtained over a 24-hour period, average temperature values obtained during the associated precipitation event, and a single snowfall observation recorded at the end of the fixed observing period. It is somewhat remarkable that the modeling results performed as well as they did given the combined impacts that significantly varying temperature and precipitation could have on snowfall production within the course of an event. Here we provide a word of caution. Use of the equations to generate hourly or even finer time-scale snowfall values that are then summed over multiple hours or even days would likely produce exaggerated and unrealistic snowfall results as was demonstrated in Section 4. An appropriate application of the models would involve the use of a distinct 24-hour bulk rendering of the water equivalent precipitation and the average of the associated temperature values observed while it was precipitating. In retrospect, the use of a weighted temperature average based on the amount of water equivalent precipitation recorded during each hour of the snowfall event might have proven more useful in the development of the models and would have likely improved the sensitivity to temperature-precipitation variations within the storm events. Another method of improving sensitivity would involve the use of a database that contained hourly snowfall and snow compaction measurements which, to the author's knowledge, does not exist.

Applying these equations to real-time automated data sets and displaying the results in a graphical interface along with verifying manual snowfall reports would be a next logical step in demonstrating the usefulness of the models in an operational setting. That said, a fairly robust automated quality control process with manual overrides would need to be implemented in order to handle or flag suspect and/or errant data. No viable method would be available to "optimize" the data stream as was done in this study since most automated platforms do not have redundant sensor packages. Finally, the snowpack is constantly undergoing metamorphosis following any snowfall event due to redistribution, compaction, melting, fragmentation, etc. (Trustman 2016, Dixon and Boon 2012, Pomeroy 1995). Additionally, the dynamic range of snow depth across spatial gradients on the order of 1 to 10 m can vary significantly (Trustman 2016, Sturm et al. 2010). The estimates generated using the proposed models are in no way meant to replace a well-seasoned observer, but would likely help to provide a reasonable depiction of ongoing snowfall events while bolstering situational awareness in an operational meteorological setting.

6. ACKNOWLEDGMENTS

Thanks go out to:

Alex DeSmet, former NWS Pocatello Meteorologist, for securing the automated observations from the Sun Valley Bald Mountain (SVB) SNOTEL site which were used in this study.

Woodward "Scooter" Gardiner from Sun Valley Bald Mountain ski operations for providing the manual observation data set from the Sun Valley resort.

Kurt Buffalo (SOO - NWS Pocatello) for his review and suggestions in the development of this paper.

7. REFERENCES

Alcott, T.I. and W.J. Steenburgh, 2010: *Snow-to-Liquid Ratio Variability and Prediction at a High-Elevation Site in Utah's Wasatch Mountains*. *Wea. Forecasting*, 25, 323–337.

Andretta, T. A. and D.S. Hazen, 1998: *Doppler Radar Analysis of a Snake River Plain Convergence Event*, *Wea. Forecasting*, 13(2), 482-491.

Baumgardt, D., D. Schmidt, and A. Just: *Environments Favorable for High Snow-to-Liquid Water Ratios across the Upper Mississippi River Valley Region*. <https://www.youtube.com/watch?v=W5gV2ZHlyt4>. October 26, 2020.

Cobb, D. K., and J. S. Waldstreicher, 2005: *A simple physically based snowfall algorithm*. Preprints, 21st Conf. on Weather Analysis and Forecasting and 17th Conf. on Numerical Weather Prediction, Washington, DC, Amer. Meteor. Soc.

Dixon, D. and Boon, S., 2012. *Comparison of the SnowHydro snow sampler with existing snow tube designs*. *Hydrological Processes* 26(17), 2555-256.

Frost, J., 2021, *Heteroscedasticity in Regression Analysis*, Statistics by Jim, Making Statistics Intuitive, statisticsbyjim.com. Accessed 3 Mar. 2021.

Frost, J., 2019, *Regression Analysis: An Intuitive Guide for Using and Interpreting Linear Models*, Statistics by Jim Publishing, State College, Pennsylvania, 331 p.

Fukuta, N., and T. Takahashi, 1999: *The Growth of Atmospheric Ice Crystals: A Summary of Findings in Vertical Supercooled Cloud Tunnel Studies*. *J. Atmos. Sci.*, 56, 1963-1979.

Georgiev G.Z., *Normality Test Calculator*, www.gigacalculator.com/calculators/normality-test-calculator.php. Accessed 1 May, 2021.

Hennemuth, B., S. Bender, K. Bülow, N. Dreier, E. Keup-Thiel, O. Krüger, C. Mudersbach, C. Radermacher, R. Schoetter, 2013: *Statistical methods for the analysis of simulated and observed climate data, applied in projects and institutions dealing with climate change impact and adaptation*. CSC Report 13, Climate Service Center, Germany.

Hultquist, T: *A Look at 6-Hour Observed Snow Ratio Climatology*. https://www.youtube.com/watch?v=LVF0CWe_0IA. October 21, 2020.

Judson, A., and N. Doesken, 2000: *Density of freshly fallen snow in the central Rocky Mountains*. *Bull. Amer. Meteor. Soc.*, 81, 1577-1587.

Krajci, P., R. Kirnbauer, J. Parajka, J. Schober, and G. Blöschl, 2017: *The Kühtai data set: 25 years of lysimetric, snow pillow, and meteorological measurements*. *Water Resour. Res.*, Vol 53, Issue 6, 5158-5165.

PennState, Eberly College of Science. *Department of Statistics. STAT 501 Regression Methods, Lesson 9 - Data Transformations*. online.stat.psu.edu/stat501/. Accessed 26 Mar. 2021.

Pomeroy, J.W., Gray, D.M., 1995. *Snowcover Accumulation, Relocation and Management*. National Hydrology Research Institute, Saskatoon, Saskatchewan, Canada.

Rasmussen, R. M., B. Baker, J. Kochendorfer, T. Meyers, S. Landolt, A.P. Fischer, E. Gutmann, 2012: *How well are we measuring snow: The NOAA/FAA/NCAR Winter Precipitation Test Bed*. *Bull. Am. Meteorol. Soc.*, 93, 811-829.

Roebber, P.J., S.L. Bruening, D.M. Schultz, and J.V. Cortinas, 2003: *Improving snowfall forecasting by diagnosing snow density*. *Wea. Forecasting*, 18, 264–287.

SkyMark. *Statistical Software Tools. Normal Test Plots*, https://www.skymark.com/resources/tools/normal_test_plot.asp. Accessed 1 May, 2021.

Sturm, M., Taras, B., Liston, G.E., Derksen, C., Jonas, T. and Lea, J., 2010. *Estimating Snow Water Equivalent Using Snow Depth Data and Climate Classes*. *Journal of Hydrometeorology* 11(6), 1380-1394.

Trustman, B., 2016: *Characterizing Spatial and Temporal Variability of Snow Water Equivalent Using Pressure Sensors*. Master's Thesis. University of Nevada, Reno. <https://scholarworks.unr.edu/handle/11714/2175>

U.S. Department of Commerce, 1996: Supplemental observations. Part IV, National Weather Service Observing Handbook No. 7: Surface Weather Observations and Reports, National Weather Service, Silver Spring, MD, 57 pp.